Finite Element Models for Dynamic Analysis of Vehicles and Bridges under Traffic Loads

Javier Oliva, Pablo Antolín, José M. Goicolea and Miguel Á. Astiz

Department Of Mechanincs And Structures. School Of Civil Engineering. Technical University of Madrid (UPM).

Abstract: We present a finite element model which takes into account the dynamic interaction between a truck and the bridge over which it is passing. The truck-bridge system presented by Marchesiello (1999) and also used by Zhu (2002) is employed to verify our model. The vehicle is a 3D truck with seven degrees of freedom. The bridge is a continuous three-span slab. The displacements obtained are very similar to the results reported by Marchesiello (1999) and Zhu (2002). Once the model has been validated the influence of road roughness is incorporated as a differential displacement between the bridge and truck wheels. Previously the road roughness is evaluated in the isolated vehicle model.

Regarding railway traffic the contact between the train wheels and the rail has some particular features which make it a highly non linear problem. In order to solve it FASTIM algorithm (Kalker, 1979) has been implemented by means of Abaqus user element subroutine for dynamic implicit analysis.

Keywords: Dynamics, Interaction, Bridges, Vehicles, Road, Railway, Roughness.

1. Introduction

When an automobile or a train passes over a bridge dynamic effects are produced in both, vehicle and structure. Those dynamic effects make the forces in the bridge increase and also affect the confort and safety of the traffic. In this work we pretend to evaluate those effects by means of finite element models. The vehicle-structure interaction is reproduced using a contact between the bridge surface and the lower nodes of the vehicle model.

2. Road traffic

2.1 Methodology

In order to verify our methodology we use a case proposed by Marchesiello (1999) that was also used by Zhu (2002) for verify their models. In that case a truck passes over a continuous three-span bridge. In Marchesiello (1999) and Zhu (2002) the bridge is modeled as a multi-span thin rectangular plate of uniform thickness and isotropic material. The deflection of the structure under the wheels is used as the input for the vehicle model as explained in Marchesiello (1999).

The viaduct (Figure 1) has a total length of 79.2 meters divided in three equal spans of 26.4 meters, a width of 10.7 m and a depth of 0.95 m. The Young modulus is $14.54 \cdot 10^{10}$ N/m^2, the Poisson modulus 0.3 and the density 2375 kg/m^3. The vehicle crosses the bridge with its right tyres at a distance of 1 meter from the structure right edge.

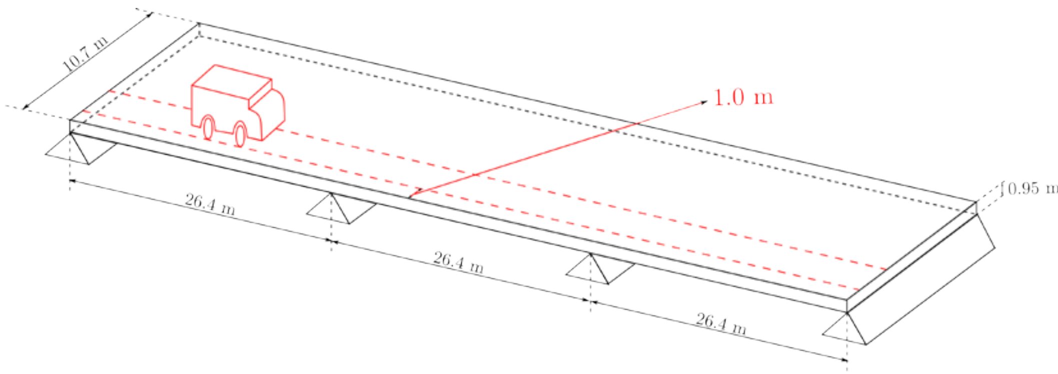

Figure 1. Sketch of the case.

The vehicle model is the one employed by Marchesiello and Zhu. It is based on the design loadings included in the *American Association of State Highway and Transportation Officials* (AASHTO) specifications and it is named H20-44. Its total mass is 18600 kg. The vehicle body is assigned three degrees of freedom (vertical displacement [y_b], pitch [β_b] and roll [α_b]) and the two axles are provided with two DOF, vertical displacement [y_{ra} for rear axle and y_{fa} for front axle] and roll [α_{ra} and α_{fa}]). The model is shown in Figure 2 and its mechanical properties are given in Table 1.

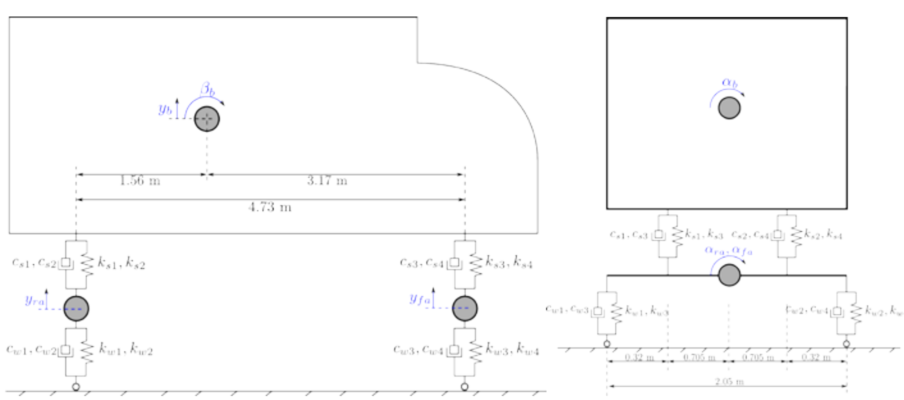

Figure 2. H20-44: side view.

Table 1. Mechanical properties H20-44.

Element	Notation	Value
Stiffnesses (N/m)		
Rear wheels	k_{w1}, k_{w2}	$1.57 \cdot 10^6$
Front wheels	k_{w3}, k_{w4}	$7.85 \cdot 10^5$
Rear suspensions	k_{s1}, k_{s2}	$3.73 \cdot 10^5$
Front suspensions	k_{s3}, k_{s4}	$1.16 \cdot 10^5$
Dampings (N·s/m)		
Rear wheels	c_{w1}, c_{w2}	200
Front wheels	c_{w3}, c_{w4}	100
Rear suspensions	c_{s1}, c_{s2}	$3.5 \cdot 10^4$
Front suspensions	c_{s3}, c_{s4}	$2.5 \cdot 10^4$
Masses (kg)		
Rear axle	m_{ra}	1000
Front axle	m_{fa}	600
Body	m_b	17000
Rotary inertias (kg·m^2)		
Rear axle roll	$I_{\alpha,ra}$	600
Front axle roll	$I_{\alpha,fa}$	550
Body roll	$I_{\alpha,b}$	$1.3 \cdot 10^4$
Body pitch	$I_{\beta,b}$	$9.0 \cdot 10^4$

2.1.1 Viaduct model

The bridge is modelled using S4R shell elements with a thickness of 0.95 m. Table 2 shows the first eight eigenvalues obtained in this work and those obtained by Marchesiello and Zhu with their thin plate models. Values are very close. Slight differences appear in the fourth, fifth and sixth frequencies that are lesser in Zhu (2002). Modes 4th to 6th are those where torsion is more important.

Table 2. Bridge natural frequencies (Hz).

Mode	This work (Hz)	Marchesiello (1999) (Hz)	Zhu and Law (2002) (Hz)
1	4.87	4.77	4.88
2	6.29	6.17	6.28
3	9.27	9.09	9.20
4	16.83	16.65	15.04
5	17.72	17.53	15.95
6	19.66	19.31	17.97
7	19.72	19.51	19.61
8	22.50	22.10	22.40

2.1.2 Vehicle model

The vehicle model is made up of rigid bodies which represent the two axles and the body, connectors that represent the wheels and suspensions, masses and rotary inertias. The eigenmodes are presented in figure Figure 3. The table shown the eigenfrequencies we have obtained and those reported by Marchesiello (1999).

Table 3. Vehicle natural frequencies.

Mode	This work (Hz)	Marchesiello (1999) (Hz)
1	0.93	0.95
2	0.93	1.06
3	1.14	1.19
4	8.73	7.69
5	9.02	8.90
6	9.94	9.54
7	12.45	12.32

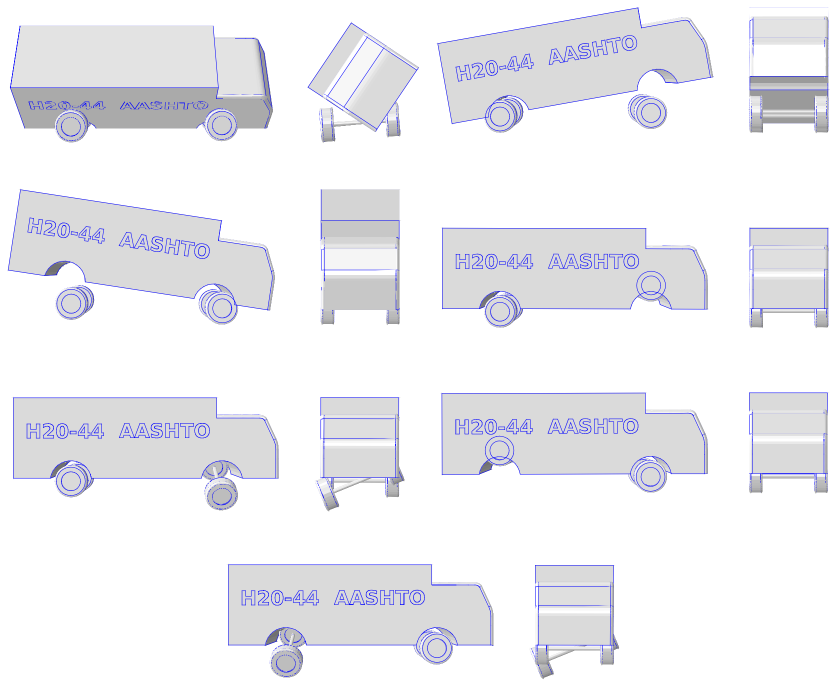

Figure 3. Vehicle eigenmodes.

2.1.3 Results

The parameter that is used to verify our model is the vertical deflection in the center of the first span when the truck crosses the bridge at two different speeds32.5 m/s and 37.5 m/s, that is, 117 km/h and 135 km/h. The values obtained by Marchesiello and Zhu are shown in Figure 4 and Figure 5 respectively. In Figure 6 our results are graphed. As can be seen values are very similar so we can conclude that the methodology we have used is suitable for representing the interaction between the vehicle and the structure.

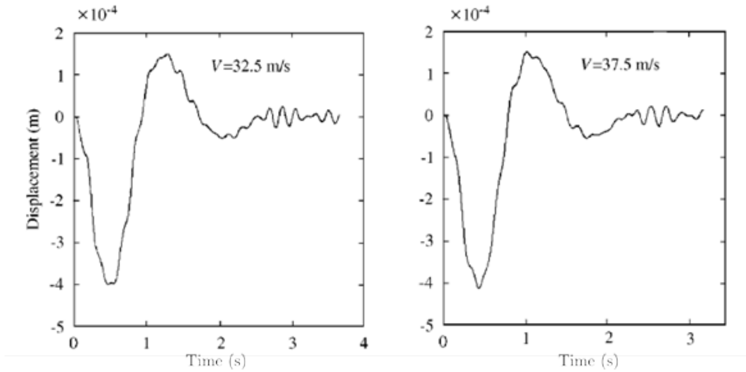

Figure 4. Vertical deflection in the first span middle point – Marchesiello (1999).

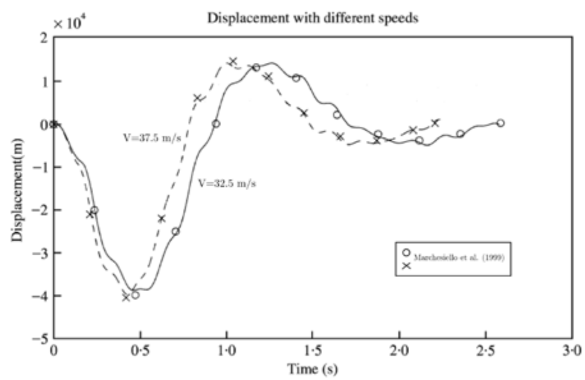

Figure 5. Vertical deflection in the first span middle point – Zhu (2002).

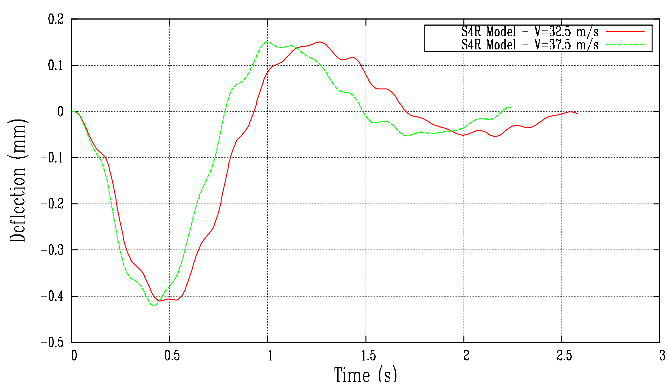

Figure 6. Vertical deflection in the first span middle point – S4R model.

2.2 Road roughness

Road surface roughness can be described through an ergodic stationary Gaussian random process described by its power spectral density, PSD. The International Organization for Standardization (ISO) proposes a definition of the one-sided PSD as a function of the one-sided PSD for a reference spatial frequency, n_0,equal to 0.1 cycles/m:

$$G(n) = G(n_0)\left(\frac{n}{n_0}\right)^{-2}$$

where $G(n)$ is the one-sided PSD for any spatial frequency (n) and $G(n_0)$ is the one-sided PSD for the reference spatial frequency (n_0=0.1 cycles/m), whose value is chosen depending on the road condition as summarized in Table 4. The road profile is generated as the sum of series of harmonics.

Table 4. *G(n₀)* ISO 8608.

Road class	$G(n_0)$ (m^3)		
	Lower limit	Geometric mean	Upper limit
A – Very good	-	$16\cdot10^{-6}$	$32\cdot10^{-6}$
B – Good	$32\cdot10^{-6}$	$64\cdot10^{-6}$	$128\cdot10^{-6}$
C – Middle	$128\cdot10^{-6}$	$256\cdot10^{-6}$	$512\cdot10^{-6}$
D – Bad	$512\cdot10^{-6}$	$1024\cdot10^{-6}$	$2048\cdot10^{-6}$
E – Very bad	$2048\cdot10^{-6}$	$4096\cdot10^{-6}$	$8192\cdot10^{-6}$

When a four-wheeled vehicle runs along a road it is subjected to four imposed displacement excitations, one at each wheel. The two wheels of the same side of the vehicle run along the same profile. But the profile under the left wheels is not the same as the profile under the right wheels. Those profiles are different but not independent. In order to define them it would be necessary to specify two direct spectral densities and two cross-spectral densities or one two-dimensional spectral density. If we accept the hypothesis that the road surface is homogeneous and isotropic its description is simplified. If we have two parallel profiles (left and right) the two PSD are the same ($G_L(n)=G_R(n)=G(n)$). The two cross-spectral densities are also the same ($G_{LR}(n)=G_{RL}(n)=G_x(n)$) and can be obtained from $G(n)$. So we have the surface described only with $G(n)$ and it is possible to generate two parallel profiles at 2.05 meters, that is the distance between left and right wheels in the H20-44 model (see Figure 7).

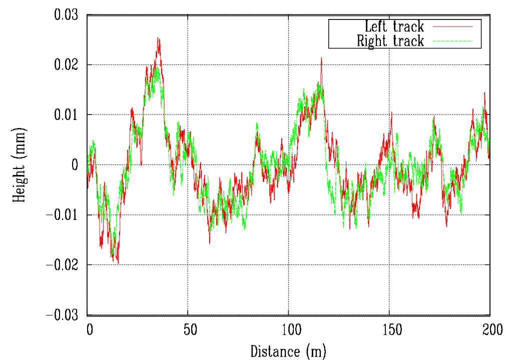

Figure 7. Parallel tracks - Distance 2.05 m - Road class B.

2.3 Vehicle running along a rough road

The results reported hereafter have been obtained considering running speeds in the range 10-110 km/h. Two 1-km-long roads are considered one of class A and one of class B according to ISO 8608. The road rougness is imposed in the vehicle in three different ways:

- The same profile at the same time for the four wheels (1p).
- The same profile for the four wheels but taking into account that the front wheels reach each point before the rear (2p).
- Different profiles for the left and the right wheels and taking into account the time difference (4p).

In Figure 8 the vertical acceleration in the vehicle body in a class A road at 110 km/h is presented as an example.

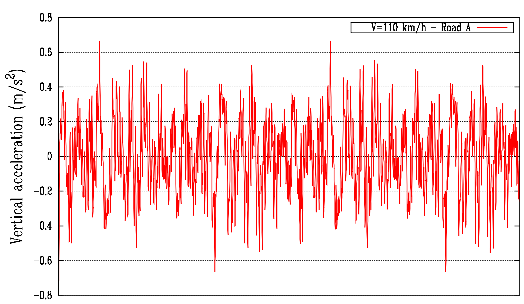

Figure 8. Vertical acceleration in the body – Road A – V=110 km/h

Figure 9 shows the root mean square (RMS) of the body vertical acceleration as a function of the vehicle speed. It is shown that the vertical acceleration increases as the speed gets higher. When the difference in the displacement excitation of the four wheels is not taken into account the values obtained are higher

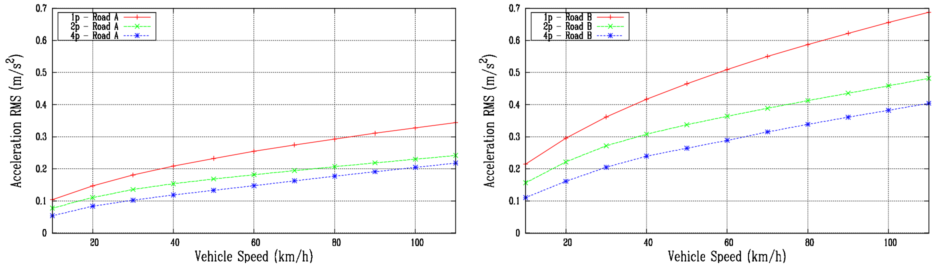

Figure 9. Vertical acceleration versus vehicle speed in a class A road (left) and in a class B road (right)

2.4 Vehicle passing over a bridge

In this section the H20-44 vehicle crosses the bridge presented in the section 2.1 at different speeds from 10 through 110 km/h. Three different scenarios are analyzed: (a) road surface has no roughness, (b) Class A road and (c) Class B road. In cases (b) and (c) road roughness has been imposed in the three different ways as in section 2.3,i.e. 1p,2p and 4p. As an example, Figure 10 shows the vertical deflection of the middle point of the first span for cases (a), (b-4p) and (c-4p).

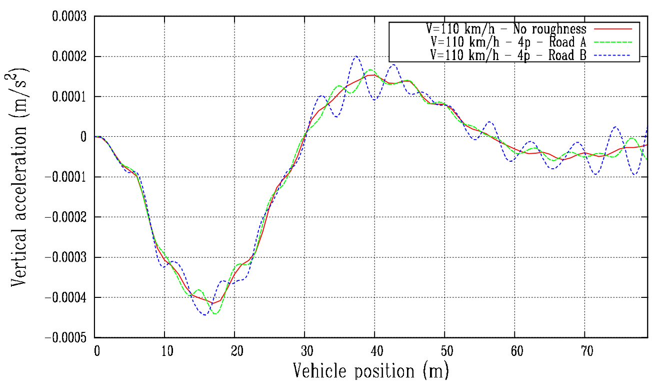

Figure 10. Vertical displacement in the first span middle point – V=110 km/h

Figure 11 shows the DAF for the vertical displacement of the first span middle point. The static deflection of that point is 0.4 mm. When no roughness is considered the maximum DAF has a value of 1.04 for a speed of 100 km/h. When road roughness is taken into account DAF gets higher reaching a maximum of 1.25 in case (c-1p) at 90 and 100 km/h. From Figure 11 we cannot come to a conclusion regarding the influence of the way in which road roughness is imposed. We have created one road profile for each case and this leads to statistical indetermination. So we need to use more profiles in order to come to a conclusion.

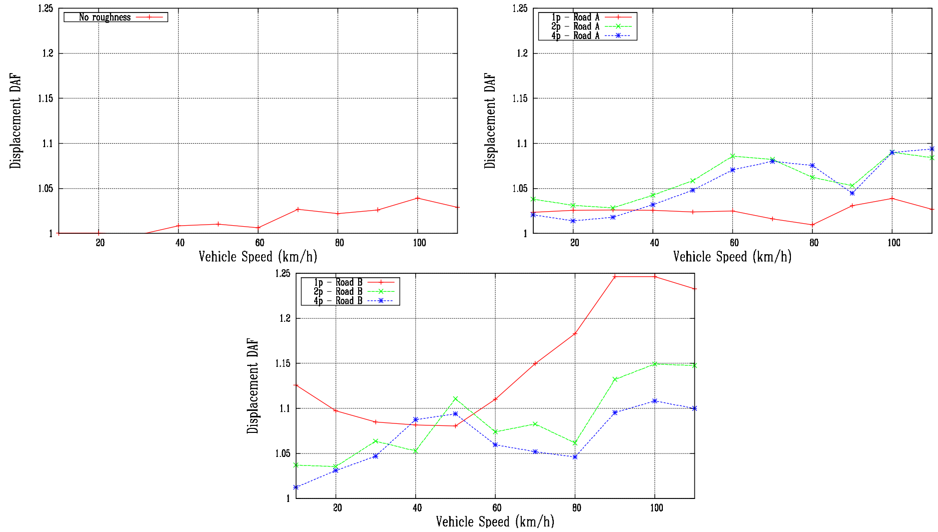

Figure 11. Displacement DAF. (a) No roughness, (b) Class A, (c) Class B.

2.5 Conclusions

It can be concluded that the Finite Element Model we have created is suitable for taking into account the vehicle-bridge interaction. Road roughness has to be considered in this kind of analysis, either for the vehicle or for the bridge, as it affects the dynamic behaviour of both. The body vertical acceleration obtained varies with the way the road roughness is introduced in the vehicle model. If the same excitation is imposed in the four wheels acceleration RMS is approximately 70 % higher. If the difference between front and rear wheels is considered and the difference between left and right wheels is neglected vertical acceleration is near 20 % higher. We need further investigation for coming to a conclusion regarding the imposition of roughness when the truck passes over the bridge.

3. Railway traffic

A railway vehicle, as in road traffic, has been modelled using rigid bodies that are associated to masses and inertias. In addition, the bodies are linked together by connectors, which simulate the behaviour of the two suspension levels of passenger railway vehicles. There has been developed a model of a vehicle with independent coaches with two bogies and two axles each, with masses, inertias and suspensions of a typical high speed train. Therefore, the model of a car has 7 rigid bodies: the car body, two bogies and four axles (Figure 12).

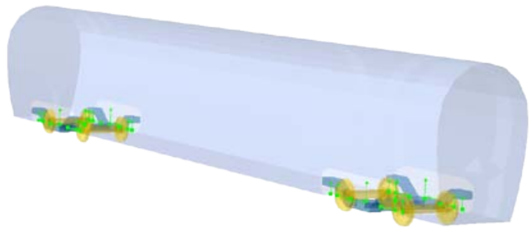

Figure 12. Railway vehicle model.

Studying vehicle-bridge interaction, to assume that coach parts are rigid body is a valid assumption. The motion of each rigid body is defined by 6 degrees of freedom (3 displacements and 3 rotations), adding up 42 variables for the whole model. Moreover, due to wheel profile, the type of rails and the separation between them and their inclination, the axles are subject to kinematic constraints that vary with wheel and rail's wear.

Kinematic constraints to be imposed to each axle have been precomputed using SIDIVE, a railway software implemented by the Spanish company CAF. Thus, the value of z and θ is determined by the value of y, lateral displacement of axle, in laws like those in Figure 13.

In the calculations, train speed is constant over the bridge, so the variable $\dot{x}$ of all the rigid bodies is constant (the train is travelling in a straight line parallel to the *x* axis), and assuming that the rotational speed of this axle is $\dot{\varphi} = \dot{x} / r_0$, where r_0 is the rotation wheel radius, assumed constant wheel (this is not true, because due to the shape profile, the radius of each wheel and varies with y), $\dot{\varphi}$ is also constant (Figure 14).

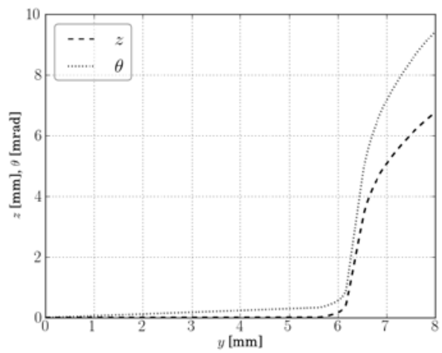

Figure 13. Kinematic constraints using a standard S1002 wheel profile and a UIC60 wheel profile.

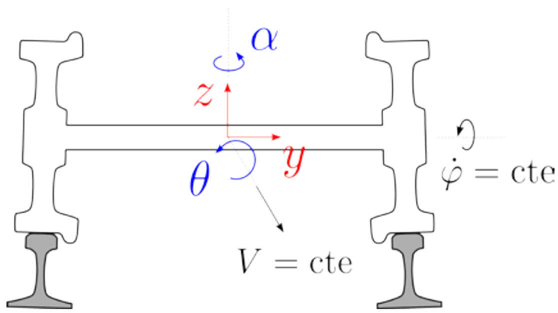

Figure 14. Degrees of freedom of vehicle axle.

In short, the number of independent variables for each axle is reduced to 2, so that the total number of degrees of freedom of the model of a car is 23 and has 8 axle kinematic constraints.

3.1 Wheel-rail contact

One of the most important points of railway dynamics is wheel-rail contact. Due to the geometric and kinematic characteristics of axles, wheels and rails, very non-linear effects appear when the vehicle goes out of its stationary regime (axle not centered between rails).

A local finite element model for relative motion between a wheel and a rail provides a good solution for their behaviour, but due to large number of elements to use this type of simulation is unfeasible to be conducted for each of the eight wheels of a coach of a train consisting of more than ten coaches running over a bridge. The time of calculation and size of the model make a simulation of this type to be unapproachable.

Thus, there are different theories to deal with the simplified form wheel-rail contact. One of the most common models used in railway dynamics programs is FastSim, proposed by J.J. Kalker (Kalker, 1982). This model solves the normal contact, through the Hertz Theory, and later, the uncoupled tangential contact with previous results.

3.2 Normal contact

The normal Hertz contact theory defines a contact surface between two bodies, with large curvature radius compared to the contact size, and similar mechanical properties, when the bodies are pressed together, as an ellipse in a plane.

Curvatures of both bodies in main directions of contact plane, which are represented in Figure 15 for any two bodies (left) and for wheel-rail pair (right), take part on ellipse dimensions.

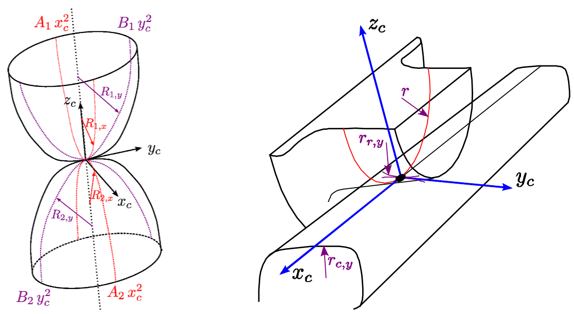

Figure 15. Left: Hertz Theory, Right: Wheel-rail pair (Iwnicki, 2006).

Due to the variation of the contact point on wheels and rails, the contact ellipse is not always contained in the same plane: the angle of the interface varies depending on y, and it is different depending on the choice of the wheel and rail and their wear (Figure 16).

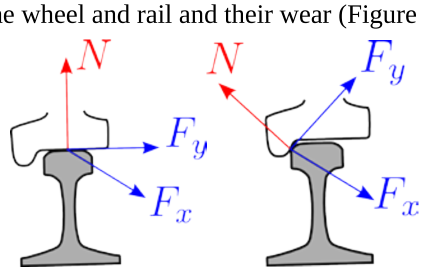

Figure 16. Contact forces during a stationary and non-stationary regimes.

Thus, taking into account the contact plane angle and imposing dynamic equilibrium of the system, it is possible to obtain the value of the normal load to the plane contact. With this value of the normal load it is possible to calculate the size of the contact ellipse.

3.2.1 Tangential contact

Once the ellipse of contact is obtained, tangential problem must be solved using FastSim. FastSim is a compromise between efficiency and an adequate accuracy solution. The main feature of FastSim is that it relates, by the Simplified Elasticity Theory, displacement and shear stresses, using the relative velocities at the point of contact between wheel and rail (creepages). So, it leads to a differential equations system that must to be solved for obtaining the shear stress distribution in two main directions of the ellipse of contact.

For solving this system it is necessary to make a discretization of the contact ellipse, like the one shown in Figure 17. These shear stresses depend on the value μ the friction coefficient, values that will vary from 0.1 for situations in which wheels and rails are wet, to values of nearly 0.5 for when both are dry.

The resultants of this distribution in the two directions are the tangential forces introduced into the finite element model of the vehicle and the viaduct.

The fundamental assumptions of this contact model are:

- normal contact is independent of the tangential,
- Hertz contact theory conditions are fullfilled,
- friction coefficient is constant throughout the contact ellipse and independent of local slip.

Moreover, this theory has been applied using the assumption that the contact in a wheel takes place at a single area, which is not always true.

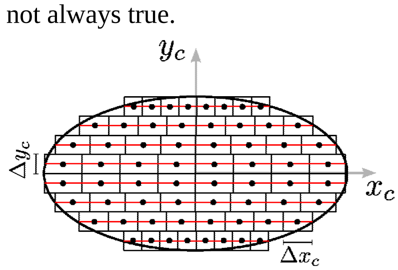

Figure 17. Discretized ellipse for solving FastSim (Iwnicki 2006).

3.2.2 Implementation

The previous wheel-rail contact has been implemented for implicit dynamic analysis by using Abaqus user subroutine for new elements.

The element has three nodes: the gravity center of the axle and the two contact points. Such points of contact also bind to the deck bridge surface by contact pairs (Figure 18). It is necessary to define a frictional user routine for obtaining the behaviour desired.

This element also impose the kinematic constraints of axis $\theta(y)$ and $z(y)$.

These constraints are included in the contact force and torque through a penalty forces:

$$F_z = k_z(z(y) - \Delta z)$$
$$M_\theta = k_\theta(\theta(y) - \Delta\theta),$$

where Δz and $\Delta\theta$ are coordinate increments normal to the bridge deck and the rotation about the axis of railway track.

Thus, at each time step, depending on the displacements and velocities of each node of the element, Hertzian contact and FastSim algorithm are solved for introducing forces on the nodes of the element. It is also necessary to calculate the stiffness and damping matrices that not having the problem an analytical solution, the Jacobians to determine these matrices in each time step must to be computed numerically.

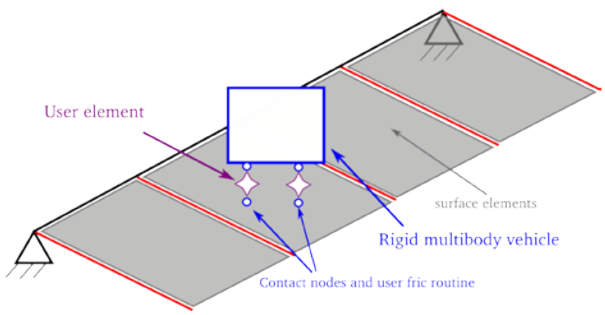

Figure 18. Vehicle-bridge interaction schema using contact user elements.

3.3 Results

Showing all of that a simulation has been performed using a single coach crossing a three span bridge (32 – 40 - 32 meters) at 200 km/h speed.

When the vehicle is over the bridge, a sudden eccentric 10 tons load is applied over the car body (it could be a wind gust) in 0.15 s and it is removed later. As can be seen in the Figure 19, lateral displacement of the car body is set in motion. As well too, a hunting movement is achieved in axles.

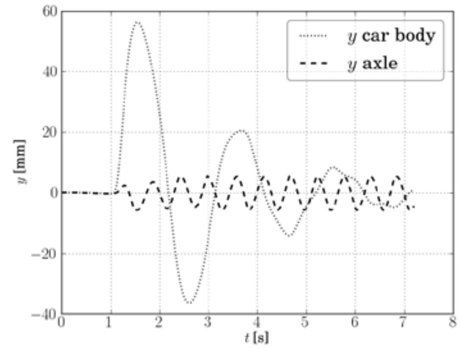

Figure 19. Lateral movement of a car body and an axle of a single coach crossing a bridge when a lateral impulsive load is acting on the car body.

3.4 Conclusions

Railway vehicle-bridge interaction introduces several differences with respect to road traffic that require special treatment. The wheel-rail contact conditions completely the train behaviour. Thus, changing conditions e.g. wear of wheels and rails, produces large variations in results. Due to problem complexity, approximate solutions, as the algorithm FastSim, are a useful way for solving the problem. It is a commitment between efficiency in the calculation and accuracy. FastSim can be implemented for vehicle-bridge interfaces using Abaqus user elements.

4. References

1. Giménez J. G., Martín L. M. and Soberano H. “Dynamic Vehicle Simulation. SIDIVE program”, Multibody Computer Codes in Vehicle System Dynamics: Supplement to Vehicle System Dynamics, 22, 1993.
2. ISO-8608. “Mechanical vibration - Road surface profiles - Reporting of measured data”, 1995.
3. Iwnicki, S. “Handbook of Railway Vehicle Dynamics”, Taylor & Francis, 2006.
4. Kalker, J.J. “Fast algorithm for the simplified theory of rolling contact,” Vehicle System Dynamics, 11:1-13, 1982.
5. Marchesiello S., Fasana A., Garibaldi L. and Piombo B. A. D, “Dynamics of multispan continuous straight bridges bridges subject to multi-degrees of freedom moving vehicle excitation”, Journal of Sound and Vibration, vol. 224, pp. 541-561, 1999.
6. Zhu X. Q. and Law S. S., “Dynamic load on continuous multi-lane bridge deck from moving vehicles”, Journal of Sound and Vibration, vol. 251, pp. 697-716, 2002.